19

Effect of plasmonic nanoparticles on generation properties dye molecules

© M.G. Kucherenko, A.P. Rusinov, F.Yu. Mushin, T.M. Chmereva

Center of Laser and Information Biophysics, Orenburg State University, Orenburg, Russia

e-mail: sano232@mail.ru Received January 31, 2025 Revised May 23, 2025 Accepted February 21, 2025

The effect of plasmonic nanoparticles (NP) on the generation of radiation by organic dye molecules has been theoretically and experimentally investigated. To calculate the intensity of radiation generated by molecules in the presence of plasmonic NPS, a theoretical model is proposed that takes into account the change in the rates of spontaneous and stimulated radiation of a molecule, nonradiative relaxation of the molecule, and light absorption by a molecule near the NPS in the velocity equations of a three-level laser. The nonmonotonic dependence of the threshold of generation of an aqueous solution of rhodamine 6G on the concentration of NPS in the solution observed in the experiment is explained on the basis of the proposed model.

Keywords: plasmonic nanoparticle, phosphor molecule, stimulated radiation, generation threshold.

DOI: 10.61011/EOS.2025.06.61668.7570-25

Introduction

The influence of plasmonic nanoparticles (NPs) on the spectral-luminescent characteristics of dyes has been actively studied both experimentally and theoretically over the past two decades. This topic is primarily interesting due to a wide range of practical applications related to the optical response of dye molecules in the presence of plasmonic NPs. For instance, principles of various modern sensors and detectors are often based on changes in the fluorescence intensity of molecules near NPs. [1-3]. It is well known that in the presence of metallic NPs, the excited-state lifetime of a molecule decreases, and fluorescence enhancement or quenching may be observed [4-6]. This is associated with the existence of localized surface plasmons in the NPs. The electromagnetic field energy of the plasmon is concentrated near the NP surface, which changes the rates of radiative and nonradiative transitions in molecules located close to the NP. Moreover, several studies [7-9] have shown that the greatest fluorescence enhancement occurs when dye molecules are located approximately $-10 \,\mathrm{nm}$ away from the

A continuing important challenge in quantum electronics is to reduce the lasing threshold and improve the emission quality of dye lasers. One approach to this problem is the incorporation of metallic NPs into the laser's active medium. Experimental studies on the influence of Ag NPs on the lasing properties of dyes in aqueous and aqueous-alcohol solutions are documented in the literature [10–13]. For example, in [10] it was shown that laser photoexcitation of aqueous rhodamine 6G solutions leads to spontaneous fluorescence, which transforms into stimulated laser emission and superluminescence with increasing pump power. The addition of Ag NPs to rhodamine 6G solutions enhances

all types of luminescence and lowers the lasing threshold for both types of stimulated emission. The presence of Ag NPs in ethanol solutions of asymmetric polymethine dyes results in an increase in emission intensity and a reduction in the lasing threshold [11]. Adding Ag NPs to ethanolic merocyanine dye solutions enables stimulated emission generation at lower pump intensities and dye concentrations compared to solutions without NPs [12]. Improved characteristics of liquid lasers based on rhodamine 640 with the addition of Au NPs to the active medium have also been reported [13].

Dye-doped solutions or polymer films containing nanoparticles serve as the active media of random lasers) [14]. These lasers lack a resonator, but a high concentration of NPs provides multiple light scattering within the active medium. As a result, photons that escape the molecular excitation zone are scattered back and amplified. The first random laser based on La₂O₃, doped with Nd³⁺ was realized by certain researchers. [15]. Later studies [16] demonstrated that the lasing threshold of rhodamine 640 in methanol with added NPs TiO₂ depends on both dye and NP concentrations, with the threshold sometimes decreasing and sometimes increasing. Numerous subsequent works have focused on random lasers with plasmonic particles. For example, in [17] it was reported that embedding Au NPs in rhodamine 6G-doped polyvinyl alcohol films leads to increased emission intensity and lowered lasing threshold. Similar results were obtained for polymethyl methacrylate films containing rhodamine 6G and Ag NPs [18], polyvinyl alcohol films with DCM dye and Au NPs [19], and polystyrene films with DCJTB dye and Ag NPs [20]. An experimental study [21] on the influence of Au, Ag, and bimetallic (Au@Ag) nanorods on stimulated emission generation of rhodamine B in polymer films showed the best lasing performance in the presence of bimetallic nanorods, which have a broad absorption spectrum largely overlapping with the absorption spectrum of rhodamine B.

As shown in several studies [22–25], the dependence of the lasing threshold on NP concentration in the active medium is non-monotonic. With increasing NP concentration, the lasing threshold first decreases and then increases. In [22] this behavior was observed for the laser dye PM597 in a nematic liquid crystal doped with Ag NPs, as well as in aqueous rhodamine 6G solutions with Au, Ag, and Pt NPs [23-25].

At low concentrations of plasmonic NPs in the active medium, where light scattering is negligible, the main physical mechanism by which NPs affect lasing generation and luminescence is the increase in radiative and nonradiative transition rates of molecules near the NPs [6,26]. At higher NP concentrations, scattering of pump and emission light by molecules is added to this mechanism, which can lead either to suppression or enhancement of laser generation [13]. It should be noted that despite numerous experimental studies on the lasing properties of dyes in the presence of plasmonic NPs, works containing theoretical analysis of the observed phenomena are significantly fewer.

This work presents theoretical and experimental results investigating the influence of gold and silver NPs on stimulated emission generation of aqueous rhodamine 6G An analysis of stationary solutions of rate equations describing the dynamics of three-level lasers was performed, accounting for changes in spontaneous and stimulated emission rates of molecules, light absorption by molecules in the presence of plasmonic NPs, and nonradiative energy transfer from excited molecules to NPs calculated within a quantum-mechanical framework. The theoretical results qualitatively explain the experimentally observed changes in spectra and lasing thresholds of aqueous rhodamine 6G solutions when plasmonic NPs are added.

Experimental Methods and Results

The experimental subject was aqueous rhodamine 6G solutions containing gold and silver NPs. The dye was chosen for its high fluorescence quantum yield and photostability. NPs were synthesized using the Turkevich-Frens citrate reduction method from aqueous tetrachloroauric acid or silver nitrate solutions. The sodium citrate aqueous solution concentration, acting as a reducing agent and metal surface stabilizer, was 80 mM, with gold and silver salt solutions at 50 mM each. Most NPs produced by this method have radii of 20-30 nm. The absorption spectra of synthesized NP solutions exhibit peaks corresponding to plasmon resonances: approximately 520 nm for gold NP solutions and 420 nm for silver NP solutions. The average NP size and total metal atom content in the reaction solution allow estimation of particle concentration at about -

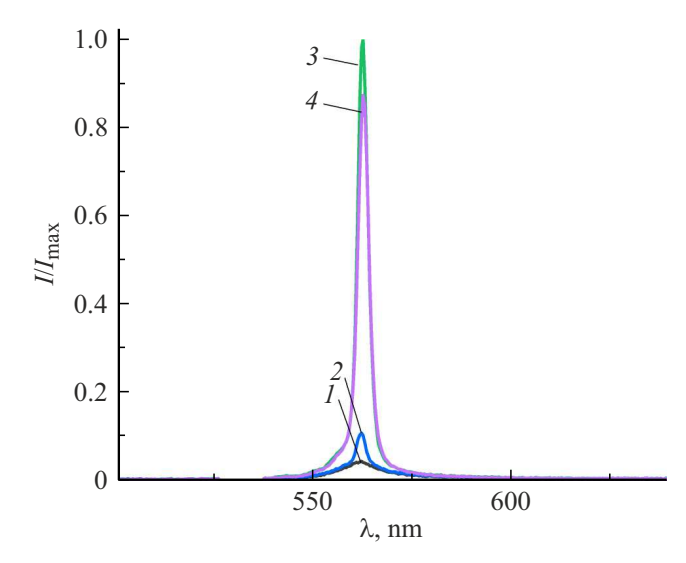


Figure 1. Emission spectra of aqueous R6G solution (1) and solutions with NPs (2-4) at a pump intensity of $210 \,\mathrm{MW/cm^2}$. The volume fractions of the NP solution in the sample were 25 (2), 37.5 (3), 50% (4).

 $5 \cdot 10^9 \,\mathrm{cm}^{-3}$. To minimize possible random lasing, it was necessary that NP solutions be weakly scattering media; therefore, synthesized NP solutions were further diluted tenfold with water.

Experimental samples of solutions were prepared with a volume of 2 ml each. One quarter of this volume was aqueous dye solution at 1 mM concentration. The rest of the sample volume was water and aqueous NP solution mixed in various proportions. Sample 1 contained no NPs; in samples 2-6 the volume fraction of diluted NP solutions increased from 0.25 ml (12.5 %) to 1.25 ml (62.5 %) in 0.25 ml increments.

In order to observe stimulated emission generation, the samples were placed in a resonator consisting of a glass cuvette with one side in contact with a back mirror and the opposite side functioning as a partially transparent mirror. Sample excitation was performed using a pulsed solidstate YAG:Nd³⁺, laser operating at 532 nm and generating 10 ns pulses. The laser intensity was varied by changing the pumping pulse duration through adjusting the time delay between powering the xenon lamp and Q-switch modulation. This parameter was varied from 90 to $200 \,\mu s$ in 10 µs steps, corresponding to laser pulse energies from 2 to 35 mJ, approximately linearly. The pump beam was focused by a spherical lens into a 1 mm diameter spot on the cuvette side perpendicular to the resonator Thus, the average intensity of the pump pulse varied in the range from 16 to 270 MW/cm². Stimulated emission generation occurred in the solution region about 0.6-0.8 mm deep from the illuminated face. emission signal was collected by a lens and, after passing through a spectrally neutral filter, registered by a CCD spectrometer BIM-6002.

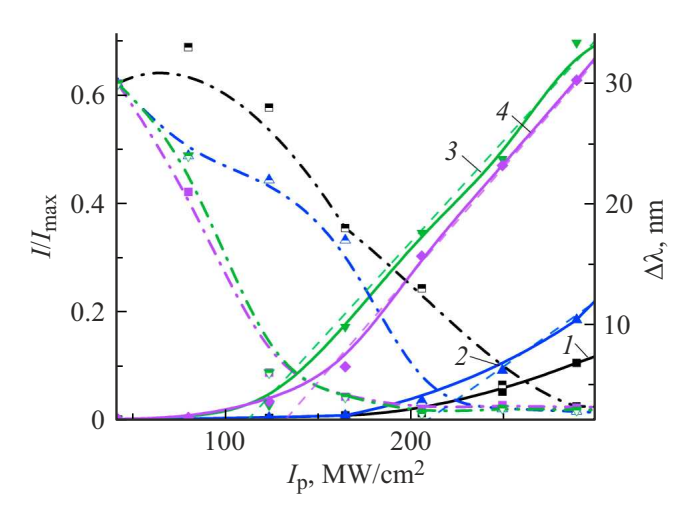


Figure 2. Dependences of the maximum intensity (solid lines) and linewidth (dashed lines) of R6G emission on pump intensity for various volume fractions of gold NPs in the sample. Curve designations are the same as in Fig. 1.

In Fig. 1, the emission spectra of gold NP samples at a constant pump intensity of 210 MW/cm² are shown. Without NPs in the solution (curve 1) dye fluorescence is observed. The presence of gold NPs in the solution leads to an increase in intensity and narrowing of the emission band (curve 2), indicating that stimulated emission of the dye dominates over spontaneous emission. the volume fraction of NPs in the solution increases, the intensity of the emission band first grows (curve 3), and then decreases (curve 4). It can be seen from Fig. 1 that stimulated emission generation occurs at the fluorescence band maximum. Similar results were obtained for silver NP samples. The reduction of emission intensity at high NP concentrations indicates that the random laser effect does not occur. Dependencies of the emission peak intensity (solid lines) and the linewidth (dashed lines) on pump intensity are shown in Fig. 2. For all samples, the emission band narrows as the excitation laser pulse intensity increases.

From the inflection point of the maxima of the emission intensity versus pump intensity graphs, the lasing thresholds for different samples were determined. As can be seen from Figs. 2 and 3, depending on the volume fraction of the NP solution, the lasing threshold behaves non-monotonically: it initially decreases and then increases, with higher emission intensity corresponding to a lower lasing threshold. A similar dependence is observed for the emission linewidth, as shown in Fig. 4.

Thus, the experiments investigated changes in the lasing characteristics of aqueous rhodamine 6G solutions with the addition of gold and silver NPs. The measurement results demonstrate a non-monotonic dependence of the lasing threshold and stimulated emission linewidth on the NP solution volume fraction in the sample, consistent with the findings of other authors [23,24].

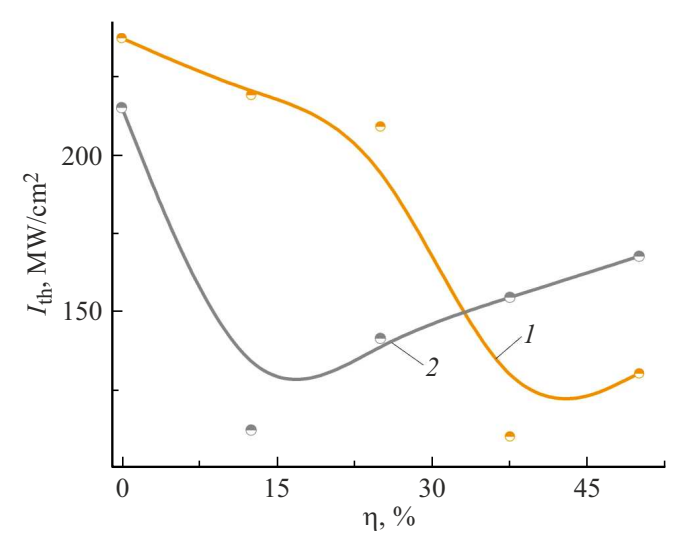


Figure 3. Dependence of the lasing threshold of R6G solutions on the volume fraction of gold NPs (I) and silver NPs (2) in the sample.

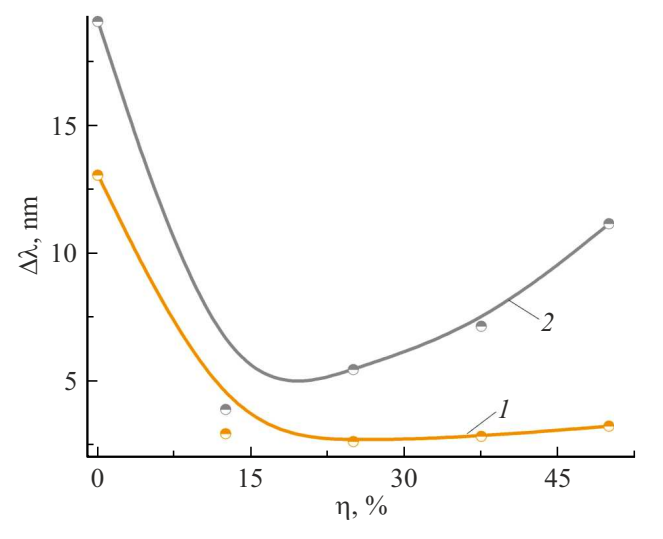


Figure 4. Dependence of the emission linewidth of R6G solutions on the volume fraction of gold NPs (I) and silver NPs (2) in the sample. Pump intensities are $210 \,\mathrm{MW/cm^2}$ (I) and $120 \,\mathrm{MW/cm^2}$ (2).

Theoretical Model and Calculation Results

The experimentally observed dependencies of emission intensity and lasing threshold on plasmonic NP concentration in the active medium are qualitatively explained using an approach based on rate equations for a three-level laser under the fast relaxation approximation [27]:

$$\dot{n}_2 = -Bn_{ph}(n_2 - n_1) - k_{21}n_2 + k_{32}n_3,
\dot{n}_3 = gn_1 - k_{32}n_3 - k_{31}n_3,
\dot{n}_{ph} = BV_a n_{ph}(n_2 - n_1) - k_{ph}n_{ph},
n_1 + n_2 + n_3 = n_0,$$
(1)

where n_0 — concentration of active molecules, n_1 , n_2 , n_3 concentrations of molecules in states 1 (ground state), 2 (upper laser level), and 3 (pump level), respectively, n_{ph} photon number in the resonator. The following notations are also used in (1): g — pump rate, B — coefficient responsible for stimulated emission or photon absorption, V_a — resonator mode volume, k_{ph} — photon decay rate in the resonator, k_{32} — nonradiative decay rate from pump level to laser level. Molecular transition rates from states 2 and 3 to ground state k_{21} and k_{31} consist of spontaneous emission rates k_{21}^r , k_{31}^r and nonradiative rates k_{21}^{nr} , k_{31}^{nr} .

The stationary solution of the rate equations system can be written as:

$$n = \frac{k_{ph}}{BV_a},$$

$$n_{ph} = \frac{k_{32}g(n_0 - n) - k_{21}((k_{32} + k_{31})(n_0 + n) + gn)}{Bn(2(k_{32} + k_{31}) + g)}, (2)$$

where $n = n_2 - n_1$ is the population inversion concentration. The spontaneous emission rate is given by [27]

$$k_{if}^{r} = \frac{4\omega_{if}^{3}\sqrt{\varepsilon}}{3\hbar c^{3}} |p_{fi}|^{2}, \tag{3}$$

where p_{fi} is the molecular transition dipole moment from an excited state i = 2 or i = 3 to the ground state f = 1, ω_{if} — the transition frequency, c — the speed of light in vacuum, ε — the dielectric permittivity of the active medium.

The pump rate can be written as $g = \sigma_{13}I_p/(\hbar\omega)$, where I_p — is the pump light intensity, ω is its frequency, σ_{13} is the photon absorption cross-section, expressed as [27]

$$\sigma_{if} = \frac{4\pi^2 \omega |p_{fi}|^2 \cos^2 \beta}{\sqrt{\varepsilon} \hbar c} \, \delta(\omega - \omega_{fi}) \tag{4}$$

at i = 1, f = 3. In (4) β is the angle between the dipole transition moment and the electric field intensity of incident wave, and, ω — frequency of incident light, $\delta(x)$ is a Lorentzian function replacing the delta function for calculations.

The value B is calculated as $B = \sigma_{12}c/V$, where V is the effective resonator mode volume, and, σ_{12} is the crosssection for the 2 and 1 laser transition at the resonator mode frequency [27] determined by the formula (4) at i = 1, f = 2.

Setting the photon number equal to zero in (2) the threshold pump rate g_{th} , can be found, and from it, the threshold pump intensity is expressed as:

$$I_{th} = \frac{\hbar \omega_{31} k_{21} (k_{32} + k_{31}) (n_0 + n)}{(k_{32} (n_0 - n) - k_{21} n) \sigma_{13}}.$$
 (5)

When a molecule is near a plasmonic NP, radiative and nonradiative electric dipole transition rates change, which alters the stimulated emission generation conditions.

In the presence of NPs, an additional relaxation channel appears: nonradiative energy transfer from excited molecules to NPs. The rate of this transfer, derived from Fermi's golden rule, is [6]

$$k_{if}^{NP}(\mathbf{r}) = \frac{4\pi^2}{\hbar\omega_p^2} \sum_{lm} \frac{\omega_l^3 (l+1)(2l+1)R^{2l+1}}{lr^{2l+4}} \times \left| \mathbf{p}_{fi} \cdot \mathbf{Y}_{lm}^{l+1*}(\Omega) \right|^2 \delta(\omega_l - \omega_{if}), \tag{6}$$

where R is the NP radius, $\mathbf{Y}_{lm}^{l+1}(\Omega)$ — a vector spherical function. The localized plasmon frequency is $\omega_l = \omega_p \sqrt{l/(\varepsilon_{\infty} l + \varepsilon(l+1))}$ (assuming the metal dielectric function given by the generalized Drude model without electron collisions) $\varepsilon_m(\omega) = \varepsilon_\infty - \omega_p^2/\omega^2$, ε_∞ — high-frequency dielectric constant, ω_p — the plasma frequency. The delta function in (3) is replaced by a Lorentzian function with halfwidth equal to twice the inverse lifetime auof the localized plasmon in the NP.

Near NPs, emission and absorption are performed by the combined "molecule + NP" system. The transition dipole moment of this system from its excited to ground state is found using a quantum-mechanical perturbation theory approach if two close energy levels are available [28]. The excited state is a superposition of two states: one with molecule excited and no plasmon in the NP; the other with molecule in ground state and one dipole plasmon in the NP. The ground state contains no plasmon and an unexcited molecule. The transition dipole moment of the combined system between the ground and excited states can be written as [28]:

$$p_{tot,m}(\mathbf{r}) = C_m p_{NP,m} + D_m(\mathbf{r}) p_{fi,m}, \tag{7}$$

where m = 0, ± 1 are the indices of the orthogonal components in the cyclic coordinate system, $p_{NP,m} = \varepsilon \sqrt{3\hbar\omega_1^3 R^3/2\omega_p^2}$ is the dipole moment matrix element of the nanoparticle (NP); $p_{fi,m}$ are the cyclic components of the molecular transition dipole moment. The coefficients $C_m(\mathbf{r})$ and $D_m(\mathbf{r})$ in equation (3) are calculated by the formulas [6]:

$$C_m(\mathbf{r}) = rac{V_{fi}(1m|\mathbf{r})}{E_m(r,\theta) - \hbar\omega_1}D_{1m}(\mathbf{r}),$$

$$D_m(\mathbf{r}) = \left(1 + \left| \frac{V_{fi}(1m|\mathbf{r})}{E_m(\mathbf{r}) - \hbar\omega_1} \right|^2 \right)^{-1/2},$$

where

$$E_m(\mathbf{r}) = rac{1}{2} \Big(E + \hbar \omega_1 \pm \sqrt{(E - \hbar \omega_1)^2 + 4|V_{fi}(1m|\mathbf{r})|^2} \Big)$$

and

$$V_{fi}(1m|\mathbf{r}) = \sqrt{\frac{12\pi\hbar\omega_1^3R^3}{\omega_p^2}} \frac{\mathbf{p}_{fi} \cdot \mathbf{Y}_{1m}^{2*}(\Omega)}{r^3}.$$

If the molecular excitation energy $E = \hbar \omega_{if}$ is less than the dipole plasmon energy $E_m(\mathbf{r})$ then in the formula for the superposition state energy one should take the lower sign;

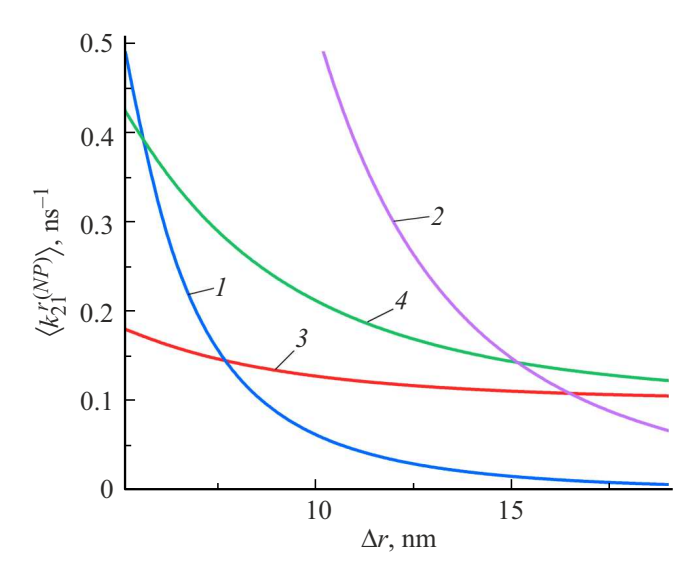


Figure 5. Distance dependencies of the angular-averaged nonradiative energy transfer rates $\langle k_{21}^{NP} \rangle$ to Ag NPs (*I*) and Au (*2*) and spontaneous emission rates $\langle k_{21}^{NP} \rangle$ near Ag NPs (*3*) and Au (*4*) as functions of the distance between the molecule and the NP surface.

otherwise, take the upper sign. Energy dissipation in the metal can be accounted for by introducing an imaginary component to the plasmon frequency $\omega_1 \rightarrow \omega_1 - i/\tau$ [28].

Thus, to determine the absorption, spontaneous, and stimulated emission rates of the molecule in the presence of NPs, in formulas (3) and (4) the molecular transition dipole moment p_{fi} should be replaced by the transition dipole moment p_{tot} of the combined "molecule + NP" system as given in (7).

Calculations based on this theoretical model were performed for silver and gold NPs with a radius of Drude parameters at optical frequencies were used: bulk plasmon energy $\hbar\omega_p = 9.0\,\mathrm{eV}$ (Ag, Au), high-frequency dielectric permittivity $\varepsilon_{\infty} = 4.45$ (Ag) and 9.8 (Au), localized plasmon lifetime $\tau_p = 40 \, \text{fs}$ (Ag) and 30 fs (Au) [29]. The dielectric constant of the active medium was $\varepsilon = 2$. The dye molecule parameters corresponded to rhodamine 6G: $\omega_{21} = 3.36 \cdot 10^{15} \,\mathrm{s}^{-1}, \ p_{12} = 6.30 \,\mathrm{D}, \ \omega_{31} = 3.54 \cdot 10^{15} \,\mathrm{s}^{-1},$ $p_{13} = 6.14 \,\mathrm{D}$. The electric field intensity of the exciting light wave and the transition dipole moment in the molecule p_{fi} were assumed parallel to the z axis of the coordinate system centered on the NP. Other model parameters were: $n_0 = 2.1 \cdot 10^{16} \text{ cm}^{-3}$, $V_a = 0.001 \text{ cm}^3$, $V = 0.0054 \text{ cm}^3$, $k_{ph} = 4.24 \cdot 10^{10} \text{ s}^{-1}$, $k_{21}^{nr} = 1.0 \cdot 10^7 \text{ s}^{-1}$, $k_{31}^{nr} = 0$, $k_{32} = 0.5 \cdot 10^{13} \text{ s}^{-1}$, $I_p = 100 \text{ MW/cm}^2$.

Figure 5 shows the distance dependencies of angular-averaged nonradiative energy transfer rates $\langle k_{21}^{NP} \rangle$ (curves 1, 2), calculated by formula (6), and spontaneous emission rates $\langle k_{21}^r \rangle$ (curves 3, 4), calculated by formula (3). The averaging was done over angular positions of the molecule near the NP surface. Curves 1 and 3 correspond to silver NPs; curves 2 and 4, to gold NPs. The figure shows that

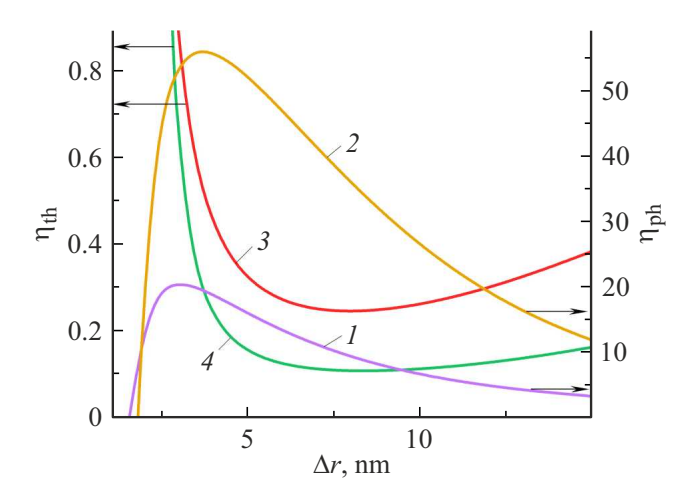


Figure 6. Distance dependencies of the ratios of generated photon numbers in the presence of Ag NPs (1) and Au NPs (2) and lasing thresholds in the presence of Ag NPs (3) and Au NPs (4) to their values without NPs.

if the distance Δr between the molecule and the silver NP surface exceeds 7.5 nm, the spontaneous emission rate becomes greater than the nonradiative relaxation rate of molecular excitation. In the range Δr from 5 to 10 nm these rates are of the same order of magnitude. For gold NPs, the corresponding range is between 10 and 20 nm. At small distances, the calculated rates for gold NPs are about an order of magnitude higher than for silver NPs, since the difference between the molecular transition frequency and the plasmon resonance frequency is smaller for gold than for silver.

Figure 6 presents the distance dependencies of the ratios η_{ph} of the numbers of generated photons calculated by formula (2), (curves 1, 2) and ratios η_{th} of the lasing thresholds, calculated using formula (5) (curves 3, 4), relative to their values in the absence of NPs. Curves 1 and 3 correspond to silver NPs; curves 2 and 4, to In the presence of NPs, the spontaneous gold NPs. emission and nonradiative relaxation rates are supplemented by the nonradiative energy transfer rate to the NP; i.e., $k_{if} = k_{if}^r + k_{if}^{nr} + k_{if}^{NP}$, i = 2, 3, f = 1. The calculations utilized angular-averaged rates of radiative and nonradiative molecular processes. From Fig. 6, it is seen that as the distance between the molecule and the NP surface decreases, the number of generated photons and the lasing threshold exhibit non-monotonic behavior. lasing threshold first decreases, then sharply increases, achieving its minimum in the distance range where the spontaneous emission and nonradiative energy transfer rates are comparable (Fig. 5). The number of generated photons first grows, then drops. This behavior is explained by the competing increase in radiative and nonradiative molecular transition rates in the presence of NPs.

Conclusion

A theoretical model of the influence of plasmonic NPs on stimulated emission generation by dye molecules is proposed. The model, based on balance equations describing a three-level laser, accounts for the effect of NPs on the spontaneous and stimulated emission rates, molecular light absorption rate, and the presence of nonradiative excitation energy transfer from molecule to NP. Numerical calculations of radiative and nonradiative transition rates in molecules located at various distances from the NP surface were performed. A distance range was established where spontaneous emission and nonradiative energy transfer rates are of the same order. It was shown that in this distance range, the lasing threshold is reduced compared to the case without NPs in the active medium.

Experimentally observed changes in the emission spectra of aqueous rhodamine 6G solutions with added silver or gold NPs are qualitatively explained on the basis of the proposed theoretical model. Low NP concentrations provide optimal average distances between molecules and nanoparticles, resulting in stimulated emission generation at pump intensities at which generation is absent without NPs. Increasing NP concentration leads to a decrease in emission intensity and an increase in lasing threshold because the average molecule—NP distance reduces and quenching of molecular excitation near NPs becomes dominant.

Thus, the conducted theoretical and experimental study shows that the greatest enhancement of emission intensity and reduction of lasing threshold occur for certain optimal geometric configurations of the "molecule + NP" system achieved at specific NP concentrations in the active medium. The results are important from an applied perspective, as improving dye lasers is a priority task in quantum electronics.

Funding

The study was supported by the Ministry of Science and Higher Education of the Russian Federation: State Order 2023-0003 for research N_2 FSGU-2023-0003 and Grant for major research projects in priority research and development areas N_2 075-15-2024-550.

Conflict of interest

The authors declare that they have no conflict of interest.

References

- M. Bauch, K. Toma, M. Toma, Q. Zhang, J. Dostalek. Plasmonics, 9, 781 (2014).
 DOI: 10.1007/s11468-013-9660-5
- [2] D.C. Mor, G. Aktug, K. Schmidt, P. Asokan, N. Asai, C.-J. Huang, J. Dostalek. Trends in Analyti-cal Chemistry, 183, 118060 (2025). DOI: 10.1016/j.trac.2024.118060

- [3] D. Semeniak, D.F. Cruz, A. Chilkoti, M.H. Mikkelsen. Advanced Materials, 35, 2107986 (2023).DOI: 10.1002/adma.202107986
- [4] A.N. Kamalieva, N.A. Toropov, T.A. Vartanyan. Proc. of SPIE, 9884, 98843C (2016). DOI: 10.1117/12.2227805
- [5] N. Ibrayev, E. Seliverstova, G. Omarova, A. Kanapina, A. Ishchenko. Materials Today: Proceedings, 71, 100 (2022). DOI: 10.1016/j.matpr.2022.09.615
- [6] T.M. Chmereva, M.G. Kucherenko, F.Yu. Mushin, A.P. Rusinov. J. Appl. Spectrosc., 91 (1), 1 (2024).DOI: 10.1007/s10812-024-01682-3
- [7] S. Murai, S. Oka, S.I. Azzam, A.V. Kildishev, S. Ishii,
 K. Tanaka. Optics Express, 27 (4), 5083 (2019).
 DOI: 10.1364/OE.27.005083
- [8] Y. Bian, S. Liu, Y. Zhang, Y. Lui, X. Yang, S. Lou, E. Wu,
 B. Wu, X. Zhang, Q. Jin. Nanoscale Research Letters, 16, 90 (2021). DOI: 10.1186/s11671-021-03546-7
- [9] D. Temirbayeva, N. Ibrayev, M. Kucherenko. J. Luminescence, 243, 118642 (2022). DOI: 10.1016/j.jlumin.2021.118642
- [10] N.Kh. Ib-rayev, A.K. Zeinidenov, A.K. Aimukhanov. Opt. Spectrosc., 117, 540 (2014).DOI: 10.1134/S0030400X14100099
- [11] N. Ibrayev, A. Ishchenko, D. Afanasyev, N. Zumabay. Appl. Phys. B, 125, 18 (2019). DOI: 10.1007/s00340-019-7292-y
- [12] D.A. Afanasyev, N.Kh. Ibrayev, G.S. Omarova, A.V. Kulinich, A.A. Ishchenko. Opt. Spectrosc., 128 (1), 61 (2020). DOI: 10.1134/S0030400X20010026.
- [13] W.Z.W. Ismail, T.P. Vo, E.M. Goldys, J.M. Dawes. Laser Phys., 25, 085001 (2015). DOI: 10.1088/1054-660X/25/8/085001
- [14] D.S. Wiersma. Nature Phys., 4, 359 (2008).DOI: 10.1038/nphys971
- [15] V.M. Markushev, V.F. Zolin, Ch.M. Briskina. ZhPS, 45 847 (1986).(in Russian).
- [16] W.L. Sha, C.-H. Lui, R.R. Alfano. Opt. Lett., 19 (23), 1922 (1994). DOI: 10.1364/OL.19.001922
- [17] O. Popov, A. Zilbershtein, D. Davidov. Appl. Phys. Lett., 89, 191116 (2006). DOI: 10.1063/1.2364857
- [18] C.T. Dominguez, R.L. Maltez, R.D. Reis, L.S.A. Melo, C.B. Araujo, A.S.L. Gomes. J. Opt. Soc. Am., 28 (5), 1118 (2011). DOI: 10.1364/JOSAB.28.001118
- [19] Y. Wan, L. Deng. Optics Express, 27, 27103 (2019).DOI: 10.1364/OE.27.027103
- [20] D. He, W. Bao, L. Long, P. Zhang, M. Jiang, D. Zhang. Optics and Laser Technology, 91, 193 (2017). DOI: 10.1016/j.optlastec.2016.12.036
- [21] A. Yadav, L. Zhong, J. Sun, L. Jiang, G.J. Cheng, L. Chi. Nano Convergence, 4, 1 (2017). DOI: 10.1186/s40580-016-0095-5
- [22] L. Ye, B. Liu, F. Li, Y. Feng, Y. Cui, Y. Lu. Laser Phys. Lett., 12, 105001 (2016). DOI: 10.1088/1612-2011/13/10/105001
- [23] V.A. Donchenko, A.A. Zemlyanov, M.M. Zinovjev, A.N. Paramonova, V.A. Kharenkov. Proc. SPIE, 10035, 1003526-1 (2016). DOI: 10.1117/12.2249339
- [24] V.A. Donchenko, A.A. Zemlyanov, M.M. Zinovjev, N.S. Panamarev, A.V. Trifonova, V.A. Kharenkov. Atmospheric and Oceanic Optics, 29 (5), 452 (2016). DOI: 10.1134/S1024856016050055
- [25] V.A. Donchenko, I.A. Edreev, A.A. Zemlyanov, V.A. Harenkov. Izv. Vyssh. Uchebn. Zaved., Fizika, 56 (8), 9 (2013) (in Russian).
- [26] A.K. Zejnidenov, N.H. Ibraev, M.G. Kucherenko. Vestnik OGU, (in Russian). 9 (170), 96 (2014).
- [27] O. Zvelto. Printsipy lazerov (Mir, M., 1990) (in Russian).

- [28] I.Yu. Goliney, V.I. Sugakov, L. Valkunas, G.V. Vertsimakha. Chem. Phys., 404, 116 (2012).DOI: 10.1016/j.chemphys.2012.03.011
- [29] V.V. Klimov. *Nanoplazmonika* (Fizmatlit, M., 2009) (in Russian).

Translated by J.Savelyeva